

2014

Flexible imaging payload for real-time fluorescent biological imaging in parabolic, suborbital and space analog environments

Matthew T. Bamsey
University of Florida

Anna-Lisa Paul
University of Florida

Thomas Graham
NASA Kennedy Space Center, Space Life Sciences Laboratory, FL

Robert J. Ferl
University of Florida

Follow this and additional works at: <http://digitalcommons.unl.edu/nasapub>

Bamsey, Matthew T.; Paul, Anna-Lisa; Graham, Thomas; and Ferl, Robert J., "Flexible imaging payload for real-time fluorescent biological imaging in parabolic, suborbital and space analog environments" (2014). *NASA Publications*. 153.
<http://digitalcommons.unl.edu/nasapub/153>

This Article is brought to you for free and open access by the National Aeronautics and Space Administration at DigitalCommons@University of Nebraska - Lincoln. It has been accepted for inclusion in NASA Publications by an authorized administrator of DigitalCommons@University of Nebraska - Lincoln.



Flexible imaging payload for real-time fluorescent biological imaging in parabolic, suborbital and space analog environments



Matthew T. Bamsey^{a,1}, Anna-Lisa Paul^a, Thomas Graham^b, Robert J. Ferl^{a,c,*}

^a Horticultural Sciences, University of Florida, Gainesville, FL 32601, USA

^b NASA Kennedy Space Center, Space Life Sciences Laboratory, FL 32953, USA

^c Interdisciplinary Center for Biotechnology Research, University of Florida, Gainesville, FL 32610, USA

ARTICLE INFO

Article history:

Received 13 May 2014

Received in revised form 25 August 2014

Accepted 18 September 2014

Keywords:

Fluorescent plant physiology imaging

Green fluorescent protein

Life support

Analog environments

Parabolic flight

Suborbital flight

ABSTRACT

Fluorescent imaging offers the ability to monitor biological functions, in this case biological responses to space-related environments. For plants, fluorescent imaging can include general health indicators such as chlorophyll fluorescence as well as specific metabolic indicators such as engineered fluorescent reporters. This paper describes the Flex Imager a fluorescent imaging payload designed for Middeck Locker deployment and now tested on multiple flight and flight-related platforms. The Flex Imager and associated payload elements have been developed with a focus on ‘flexibility’ allowing for multiple imaging modalities and change-out of individual imaging or control components in the field. The imaging platform is contained within the standard Middeck Locker spaceflight form factor, with components affixed to a baseplate that permits easy rearrangement and fine adjustment of components. The Flex Imager utilizes standard software packages to simplify operation, operator training, and evaluation by flight provider flight test engineers, or by researchers processing the raw data. Images are obtained using a commercial cooled CCD image sensor, with light-emitting diodes for excitation and a suite of filters that allow biological samples to be imaged over wavelength bands of interest. Although baselined for the monitoring of green fluorescent protein and chlorophyll fluorescence from Arabidopsis samples, the Flex Imager payload permits imaging of any biological sample contained within a standard 10 cm by 10 cm square Petri plate. A sample holder was developed to secure sample plates under different flight profiles while permitting sample change-out should crewed operations be possible. In addition to crew-directed imaging, autonomous or telemetric operation of the payload is also a viable operational mode. An infrared camera has also been integrated into the Flex Imager payload to allow concurrent fluorescent and thermal imaging of samples. The Flex Imager has been utilized to assess, in real-time, the response of plants to novel environments including various spaceflight analogs, including several parabolic flight environments as well as hypobaric plant growth chambers. Basic performance results obtained under these operational environments, as well as laboratory-based tests are described. The Flex Imager has also been designed to be compatible with emerging suborbital platforms.

© 2014 The Committee on Space Research (COSPAR). Published by Elsevier Ltd. All rights reserved.

1. Introduction

There are strong scientific and engineering justifications for deploying non-destructive biological imaging systems in spaceflight environments. In the near term, these imaging systems will help reveal the effects of the spaceflight environment on biological systems and the responses required to adapt to spaceflight environments. Proper imaging systems can provide real-time, macroscopic-level data on the response of biology to the spaceflight environment. These systems are also capable of delving deeper into spaceflight effects by providing information on responses at the gene expression level (Paul et al., 2013, 2012). This information serves to improve our fundamental understanding of

Abbreviations: ABRS, Advanced Biological Research System; ACMG, Arthur Clarke Mars Greenhouse; BPS, Biomass Production System; CCD, Charge-coupled device; COTS, Commercial off-the-shelf; CSA, Canadian Space Agency; CWL, Central wavelength; EMCS, European Modular Cultivation System; FWHM, Full-width half-maximum; GFP, Green fluorescent protein; GIS, GFP Imaging System; ISS, International Space Station; LED, Light-emitting diode; M-PHIS, Multispectral Plant Health Imaging System; MDL, Middeck Locker; NASA, National Aeronautics and Space Administration; NPP, NASA Postdoctoral Program; OD, Optical depth; PAR, Photosynthetically active radiation; TAGES, Transgenic Arabidopsis Gene Expression System; TIS, TAGES Imaging System.

* Corresponding author. Tel.: +1 352 273 4822.

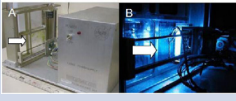


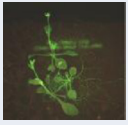


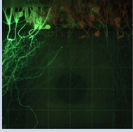

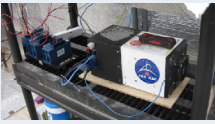


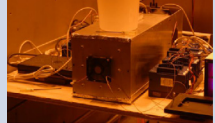
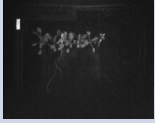

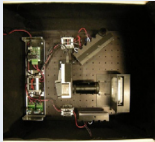


¹ Present address: German Aerospace Center (DLR), Institute of Space Systems, Bremen, D-28359, Germany.

<http://dx.doi.org/10.1016/j.lssr.2014.09.002>

2214-5524/© 2014 The Committee on Space Research (COSPAR). Published by Elsevier Ltd. All rights reserved.

Table 1

University of Florida collaborated GFP imaging system historical development summary. TIS = TAGES Imaging System, TAGES = Transgenic Arabidopsis Gene Expression System, M-PHIS = Multispectral Plant Health Imaging System. The environments for deployment of the imagers are 1 = Arthur Clarke Mars Greenhouse, 2 = ISS, 3 = parabolic flights (KC-135, 727-200), 4 = hypobaric chamber, 5 = T-6 flights, 6 = suborbital flight.

Name	Hardware	Sample Image	Test Environment	Ref.
TIS-I 2000–2003				Paul et al. (2003)
TIS-II 2004–2006			1 	Paul et al. (2008)
GIS GIS-III or GFP-III 2007–Present			2 3 	Paul et al. (2012, 2013)
TIS-III 2009–2011			1 	Abboud et al. (2013b)
TIS-IV 'M-PHIS' 2010–2012			4 	Abboud et al. (2013a)
TIS-V 'Flex' 2013–Present			3 4 5 6 	Presented herein

how biology responds to the evolutionarily novel environmental conditions associated with spaceflight (e.g. microgravity, radiation, pressure).

Imaging of plants in spaceflight applications is particularly important when considering the long-term engineering requirements for bioregenerative life support systems. The use of crop health imaging hardware will contribute to the optimization of the plant growth environment through the provision of biologically relevant feedback data that will feed into the environment control system. Similarly, these imaging systems will contribute to the overall reliability of the life-support system through early detection of non-optimal plant metabolism (Knott and Sager, 1991).

Historically, fluorescent imaging of plant health has been centered on the variations that can occur in natural chlorophyll fluorescence (Krause and Weis, 1991; Maxwell and Johnson, 2000). More recently, modern molecular techniques have made available a range of fluorescent molecules that can be incorporated as genetic reporters of specific and wide ranging biological responses to stimuli/stress (Zhang et al., 2002). These responses can be characterized through the use of imaging hardware incorporating appropriate excitation and imaging wavelengths. The use of Green Fluorescent Protein (GFP) and its variants as biosensor molecules has served as a valuable tool in several such imaging systems (Paul et al., 2013; Stewart, 2001). Although commercial imaging systems do exist for GFP imaging, the typical configuration of these systems (e.g. mass, volume, mechanical design, etc.) preclude their use within the sub-orbital or orbital environment, thereby necessitating the development of custom imaging systems such as those described herein.

A wide array of imaging systems have been developed and utilized for the telemetric monitoring of plant experiments on the International Space Station (ISS). Systems have been incorporated into both temporarily and permanently installed ISS plant growth hardware such as Advanced Astroculture (Link et al., 2003; Zhou, 2005), Biomass Production System (BPS) (Morrow and Crabb, 2000; Stutte et al., 2005), Plant Generic Bioprocessing Apparatus (PGBA) (Hoehn et al., 1996; Evans et al., 2009), Lada (Sychev et al., 2007; Bingham et al., 2003), European Modular Cultivation System (EMCS) (Brinckmann, 2005; Johnsson et al., 2009), Biolab (Brinckmann, 2005) and the Green Fluorescent Protein (GFP) Imaging System (GIS) within the Advanced Biological Research System (ABRS) (Paul et al., 2012; Levine et al., 2009). Visible light imaging has been implemented in the bulk of these plant growth chambers, but monitoring has also been conducted through infrared and fluorescent means.

Several fluorescent imager designs have been developed in the past decade, using spaceflight and related environments as the overarching design thrust. These systems were each designed to meet the specific criteria relevant to their particular application or deployment environment (Table 1). These imagers have been deployed in one or more of the following environments; laboratory (Paul et al., 2003, 2008, 2012, 2013; Abboud et al., 2013a, 2013b), autonomous greenhouse in a remote environment (Paul et al., 2008; Abboud et al., 2013b), hypobaric plant growth chamber (Abboud et al., 2013a), parabolic flights, and aboard the Space Shuttle and ISS (Paul et al., 2012, 2013; Levine et al., 2009).

The development and operation of these imagers in their various space and space-related test environments have resulted in a

Table 2

Top level requirements used in the design of the Flex Imager and summary of the primary method incorporated into the design to address each requirement.

Top level requirement	Primary method used to address requirement
Mechanical integration in a wide array of flight vehicles	MDL sizing
Flexible component positioning	Multi-hole baseplate
Capacity for field replacement/upgrade of individual components	COTS cameras, lenses and other hardware
Support a broad range of biological imaging samples	Filter wheel with multiple imaging filters, accommodate standard 10 cm × 10 cm Petri plate samples
Broad range of acceptable input power	Selection of power components with wide input voltage ranges
Ease of programming and autonomy	COTS software
Possibility for rapid analysis of collected imaging and environmental data	Common software packages and formats

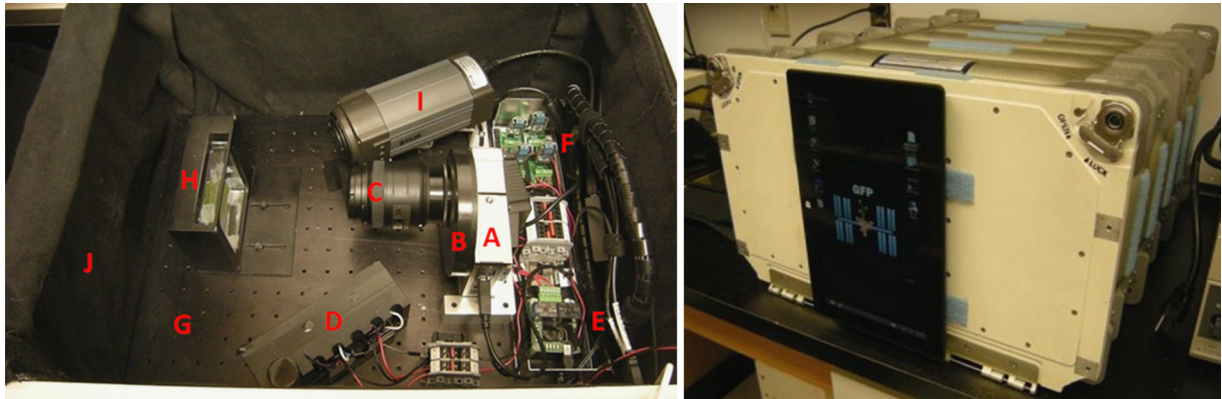


Fig. 1. Flex Imager internal payload configuration (left) and external MDL configuration (right) utilized in the T-6 flight campaigns. Monochrome camera (A), filter wheel (B), F-mount lens (C), excitation filter/LED enclosure box (D), USB controlled relays (E), voltage regulators (F), baseplate (G), sample holder and installed sample (H), infrared camera (I), block-out cloth (J).

number of enhancements that will further the capacity of future imagers to collect real-time fluorescence information from plants and other organisms as they respond to novel environments. This, in addition to potential flight opportunities on upcoming suborbital vehicles, led to the development of the TIS-V, or the Flex Imager. The Flex Imager focuses on a ‘flexible’ design in which the imager can be easily adjusted to different development pathways and rapid reconfiguration in field deployments. Specifically, it employs a modular design that permits the replacement of individual components as new and improved technologies come online. From this perspective, unlike many other imager designs that have been specific application driven, the Flex Imager relies heavily on commercial off-the-shelf (COTS) parts. This enables the modularity of the imager while reducing the learning curve for new operators of the system.

Parabolic and suborbital platforms have the luxury that they offer researchers and hardware developers multiple flight opportunities into which flight experience can be incorporated into future flights. Flexible payloads can take even greater benefit in these multiple flight opportunities in that, researchers can rapidly incorporate hardware refits to maximize scientific and/or technology maturation return in subsequent flights (e.g. even in the same day). As the Flex Imager was designed with various parabolic and suborbital flight platforms in mind, there has been an impetus to reduce overall mass, volume and power requirements of the system while conforming to a standard Middeck Locker (MDL) (NASA, 1984; Boeing, 1997) form factor while simultaneously enabling rapid refit and reconfiguration between flights.

2. Flex Imager design

2.1. Design rationale

The basis of the Flex Imager concept is the flexible use of the volume within a standard MDL. The MDL is nearly ubiquitous in spaceflight payload development and it is supported by many

of the newer generation of suborbital vehicles. Use of the MDL retains strong spaceflight heritage while presenting enough volume for accommodating many modern commercial imaging components. One key aspect is the development and installation of a baseplate that allows multiple component localizations within the MDL, with each component then adaptable to flexible localization on the baseplate. Those additional components are the modularized imaging camera and lens, power supplies, excitation light sources, and sample holders. Furthermore, the flexible configuration permits simplified field replacement of non-functional components or eases module reconfigurations within the payload. Replacement and reconfiguration are both of high benefit with the increased flight rate that suborbital vehicles are expected to provide. Although deployed for the fluorescence imaging of *Arabidopsis*, the Flex Imager was developed with provision to provide a more generic platform capable of imaging any biological science sample that can be contained within a standard laboratory 10 cm × 10 cm Petri plate. The top level design criteria used to develop the Flex Imager as well as the primary manner in which each requirement was addressed (e.g. COTS hardware) are summarized in Table 2.

The Flex Imager including its various subsystems; imaging system, filters, lighting system, mechanical, power and control system and software have each been influenced by the aforementioned design requirements. The internal configuration of the Flex Imager as well as its ready-to-deploy MDL configuration with optional externally mounted interface tablet are shown in Fig. 1.

The current Flex Imager configuration shown in Fig. 1 has evolved based upon laboratory and flight and analog deployment experience. Earlier configuration details, when relevant, are provided in latter sections on imager testing and deployment descriptions. Also of note is that the current configuration of the Flex Imager incorporates an infrared imaging system. Although not explicitly considered part of the Flex Imager, the thermal camera provides important ancillary data to further validate the fluorescence

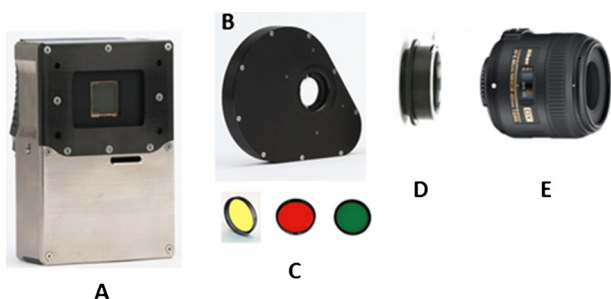


Fig. 2. The primary imaging components of the Flex Imager including an Ascent A8050 monochrome camera, six position filter wheel, installed filters, F-mount lens and associated adapter. A = camera, B = filter wheel, C = imaging filters, D = lens mount, E = lens. Image credits: Apogee Imaging Systems and Nikon USA.

imaging results and has been incorporated to provide a supplemental tool for additional biological science investigations.

3. Imaging system

The Flex Imager was built around an Ascent A8050 monochrome camera from Apogee Imaging Systems (Roseville, California). The 16 bit digital resolution A8050 has a 3296×2472 pixel Kodak KAI-0850 CCD ($4/3''$ optical format). A primary driver for the selection of this camera was that it incorporated a thermoelectrically cooled image sensor. From past parabolic flight experience, it was determined that stabilized CCD temperatures would permit more consistent imaging and maintaining the CCD at low temperatures would permit improved imaging results. The Flex Imager also included a CFW25-6R six position compact filter wheel from Apogee Imaging Systems and an AF-S DX Micro-NIKKOR 40 mm f/2.8G close-up lens from Nikon (Melville, New York). To permit the installation of the F-mount Nikon lens onto the filter wheel, a 300658 Apogee Imaging Systems adjustable Nikon to CFW25-6R adapter was utilized. Filters were installed into five out of the six filter wheel positions. The basic imager configuration is illustrated in Fig. 2.

The incorporation of the filter wheel was based upon the desire to monitor chlorophyll fluorescence and additional fluorescent proteins over and above GFP. Although a liquid crystal tunable filter had been utilized in the earlier TIS-IV (Abboud et al., 2013a), a filter wheel was chosen in lieu of this option due to the limited out of band blocking (average $> OD2$) that was achieved with the tunable filter. Although the filter wheel limited the number of potential filtering possibilities, it provided the operator with consistent, well characterized filters with high out of band blocking (typical $> OD4$). The CFW25-6R filter wheel was chosen as it was directly developed for use with the Ascent series cameras and is provided with data and power through a dedicated port on the camera (Ascent Peripheral Interface). Also of importance, was the fact that the filter wheel could be operated through the same control software as the camera. In addition to being typically more appropriate for large CCDs, an F-mount lens was utilized due to the fact that with the 19.7 mm thickness of the filter wheel, the flange to focal plane distance of a C-mount lens (17.526 mm) was insufficient. Instead, an F-mount lens with its flange to focal distance (46.5 mm) matched the sum of the F-mount lens to filter wheel adapter height (~ 18 mm), filter wheel thickness (19.7 mm) and back focal distance of the Ascent camera (8.1 mm). When utilized for in flight or laboratory-based imaging, the lens object distance setting was adjusted to approximately 0.3 m, the aperture was set close to fully open and the lens was threaded out from fully installed, by an approximate 0.5 to 1 full turn. When these settings were applied, the camera obtained focused images with the sample holder installed approximately 13 cm to 16 cm away when

measured from the front face of the lens. In this configuration the focus was fixed and the operator could not, through software, adjust the focus in flight. A monochrome camera was selected for the Flex Imager due to the known spectra of the various filters and the improved spatial resolution and overall quantum efficiency of the CCD.

4. Filters

The Flex Imager incorporated an excitation filter and five imaging filters. The excitation filter was installed between the excitation LEDs and the sample, while the imaging filters were installed within the filter wheel between the sample and the camera CCD. An empty filter wheel position was kept for white light imaging.

4.1. Excitation filter

The Flex Imager's excitation filter was based upon the same excitation filter utilized in the on-orbit GIS imager (Paul et al., 2012, 2013). It was fabricated from a 3.2 mm thick $5'' \times 5''$ spare version of the on-orbit GIS imager filter that was cut into two equal rectangular pieces by the Canadian Space Agency machine shop. One of these $2.5'' \times 5''$ pieces was installed within the Flex Imager. This sizing was selected as the Flex Imager was initially being designed to be housed in a half MDL tray, which has a maximum height of approximately 4.25''. The 480 nm bandpass filter (part number D480/10X) was acquired from Chroma Technology Corp. (Rockingham, Vermont) and had the following specifications; central wavelength (CWL) of $480 \text{ nm} \pm 4 \text{ nm}$, full-width half-maximum (FWHM) of 10 nm and an average out of band blocking (300–1200 nm) of OD6 (minimum OD5).

4.2. Imaging filters

Employed imaging filters were acquired from Omega Optical (Brattleboro, Vermont). The purpose of each filter and their basic optical and operational specifics (e.g. filter wheel location, integration time) are provided in Table 3. Each of the listed filters had out of band blocking greater than OD4 and were of 25 mm diameter construction.

5. Excitation lighting system

Fluorescence excitation light was provided by two 40 mm circular LED assemblies from Luxeon Star LEDs/Quadica Developments Inc. (Brantford, Ontario). The 470 nm centered blue LED assemblies (SR-02-B0040) providing 490 lm at 700 mA each incorporated seven 2 W LXML-PB01-0040 Philips Rebel LEDs. As these LEDs had a 125° viewing angle ($2\theta_{1/2}$) the LED assemblies were covered with a polycarbonate collimator that resulted in a diffused output with an approximate viewing angle of 12° (Polymer Optics 7 LED Cell Cluster 12° Diffused Optic Array from Luxeon Star LEDs/Quadica Developments Inc.). The diffused version of the collimator was selected to produce a more evenly distributed beam on the biological sample. Two 40 mm 470 nm LED assemblies each with six LEDs wired in series, were utilized to provide excitation light for imaging. Each LED assembly was wired to an A011-D-V-700 FlexBlock constant current driver from LEDdynamics, Inc. (Randolph, Vermont). These constant current drivers were wired in buck-boost mode and provided each series of LEDs with 700 mA.

The two Flex Imager excitation LED boards were housed behind the $2.5'' \times 5''$ excitation filter in a custom fabricated aluminum enclosure. The enclosure box, described in more detail in a later section, provided a stable mounting surface and was built large enough to limit and help regulate LED temperature. Thermal tape

Table 3
Flex Imager imaging filters basic specifications.

Position	Product name	Type	Imaging purpose	CWL (nm)	FWHM (nm)	Integration time (s)
1	3RD510LP	Longpass	Green to red fluorescence	510 (cut-on)	N/A	1
2	515BP10 (custom)	Bandpass	Green fluorescence	515	10	10
3	520BP10	Bandpass	Green fluorescence	520	10	10
4	660DF10	Bandpass	Red fluorescence	660	10	10
5	730AF45	Bandpass	Near IR fluorescence	730	45	5
6	Empty	N/A	White light	N/A	N/A	0.025

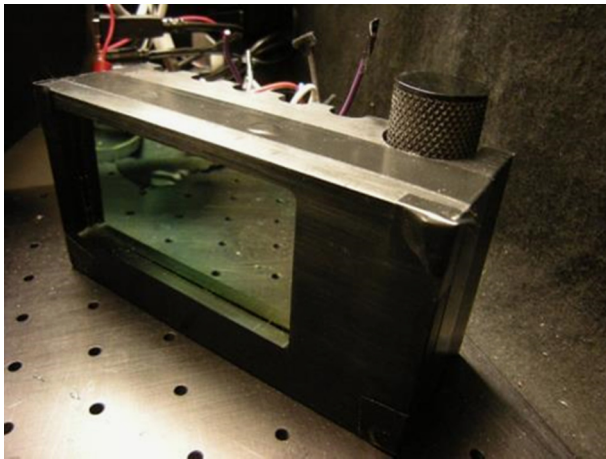


Fig. 3. Completed excitation filter/LED enclosure box showing filter covering the windowed entry into box. The two LED excitation boards (not visible) were installed inside the enclosure box.

(electrically isolating) cut to the appropriate size was installed behind the LED boards to increase heat conduction to the enclosure box and three screws were used to mount the boards in position in the prescribed location. To reduce light reflection within the MDL drawer, hardware was anodized or painted matte black when possible. All interior surfaces of the MDL tray were covered with a velcroed layer of black duvetyne cloth. A layer of cloth was also strung across the top of the tray for the same purpose.

6. Mechanical design

The mechanical design of the Flex Imager focused heavily on flexibility. As part of the imager development, a flexible baseplate was designed in conjunction with Earthrise Space (Orlando, Florida). This aluminum (6061-T6) baseplate was sized to fit the foot-print of a nominal MDL tray and was 19" × 14-1/4" in size. It had a 1" × 1" hole pattern (10–32 threads) over the entire surface and was of 1/4" thickness to provide solid mounting while permitting component change-outs, relocation and reorientation. To minimize mass, the baseplate was isogrid on the underside. Imager components were developed to mount to the Flex Imager baseplate directly through 10–32 mounting bolts or with adapters accepting such a bolt pattern and thread definition. The basic layout of the Flex Imager including mechanical components is displayed in Fig. 1.

An excitation LED and filter enclosure box was fabricated in conjunction with Earthrise Space and served to house the two circular excitation LED assemblies, associated collimators and the excitation filter. The completed enclosure box with installed excitation filter is shown in Fig. 3. To provide future design flexibility, the enclosure box was designed to accept filter thicknesses as low as 1.0 mm and up to 5.0 mm. No active cooling of the LEDs was utilized as the thermal mass of the enclosure box itself provided ample passive cooling to maintain the LEDs within their operational temperature bounds. This was particularly made possible because the

LEDs were only activated for short and discrete periods during image collection. The hand tightened gnarled tie-down bolt (in Fig. 3) was used to securely mount the enclosure box to the baseplate.

As the primary imaging target of interest was biology contained in nominal 10 cm × 10 cm Petri plates, a biological sample holder was developed to permit secure mounting of these plates for flight while also allowing easy sample change-out (i.e. during flight). To permit flexibility and optimize image quality, the sample holder was designed to include a slotted mount to allow rapid and fine repositioning of the sample along the axis of the camera. A lightweight camera mount designed by the University of Florida and fabricated by TMR Engineering (Micanopy, Florida) was used to mount the camera and its associated filter wheel and lens to the baseplate. A COTS 12" × 3" × 2.3" aluminum enclosure box (1411WU) from Hammond Manufacturing (Guelph, Ontario) was acquired and installed to house power and control system components (USB relays, DC–DC converters and imager terminal blocks).

7. Power and control system

Although the Flex Imager was designed with primary consideration of use with typical 28 VDC supply voltages of sub-orbital vehicles currently under development (XCOR-Aerospace, 2012; Virgin-Galactic, 2011) (and on upon past Space Shuttle payload supply voltage), power management components were chosen to broaden acceptable input voltages. The Flex Imager could accept a supply from 15 VDC to 28.5 VDC. To supply the Ascent camera with its required 6 VDC, two DE-SWADJ 3 A adjustable voltage regulators from Dimension Engineering (Akron, Ohio) were employed. Despite the fact that a single 3 A regulator would have provided adequate, two regulators were wired in parallel to ensure that at high thermoelectric cooler power levels, that the camera would be provided with sufficient power while not overheating either regulator. Additional DE-SWADJ 3 A regulators were installed to power the infrared camera (12 VDC) and Belkin USB hub (5 VDC).

Other powered components included the LEDs which, were powered using constant current drivers fed directly from the Flex Imager supply voltage. The two USB controlled relays utilized to control the on/off of the excitation LEDs and thermal camera were powered directly (5 VDC) through the USB port for which they were connected to the operations computer. These custom USB powered 2-channel relay controller boards were acquired from National Control Devices (Osceola, Missouri). The general wiring layout of the Flex Imager is displayed in Fig. 4.

The four DE-SWADJ 3 A regulators were installed on small voltage regulator breakout boards offered by Dimension Engineering. The regulators could accept input voltages between 5 V and 33.6 V while providing adjustable output between 3 V and 13 V. These lightweight regulators (10 g) had a max rating of 25 W or 3 A.

One FlexBlock was utilized for each 40 mm LED assembly and the FlexBlock units were installed on the outside of the back of the aluminum LED enclosure box. Thermal tape was used to increase heat transfer and connecting wires were passed through predrilled wiring ports at the back of the enclosure box. The FlexBlock was wired in buck–boost configuration. The flexible buck–boost configuration allows the input voltage to be less than, the same, or

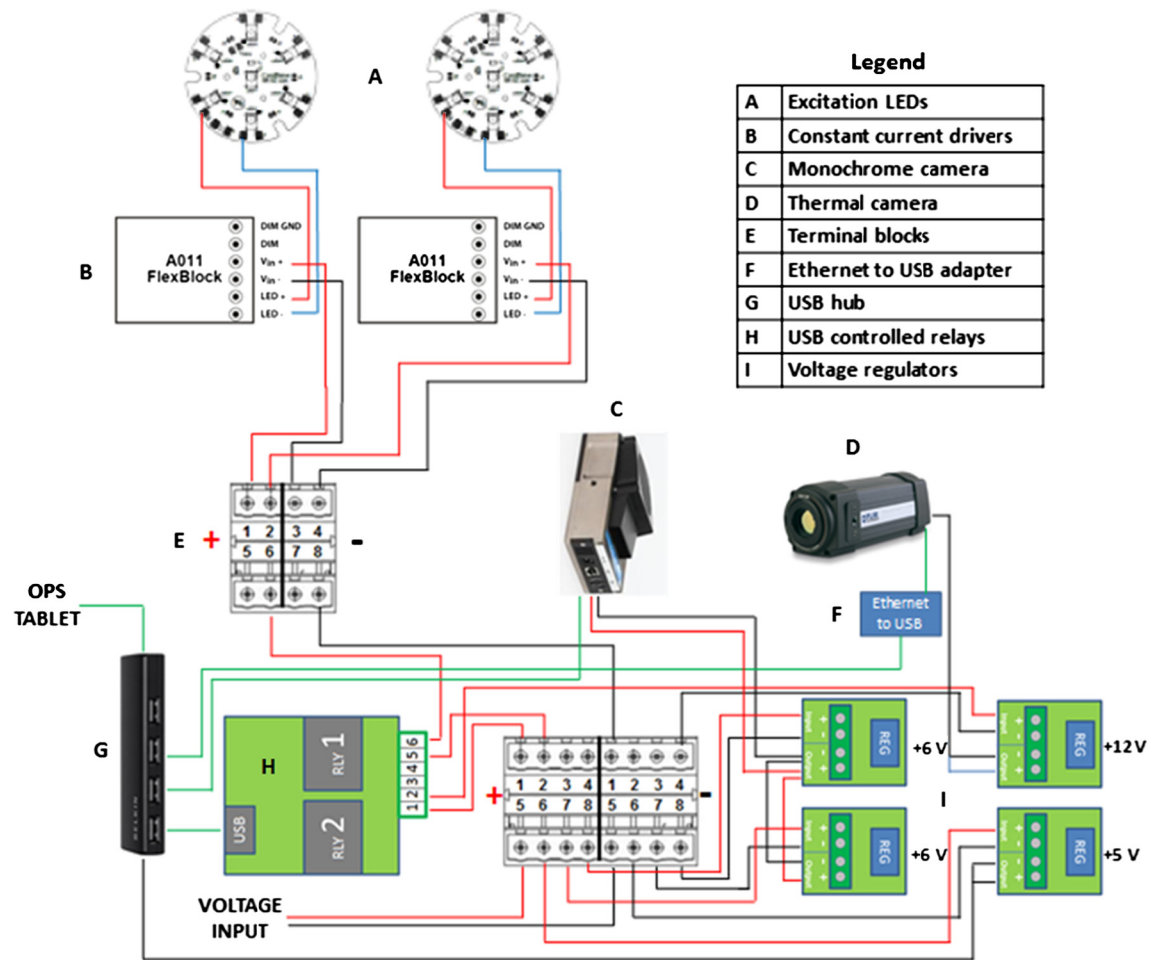


Fig. 4. Flex Imager graphical wiring diagram.

greater than the output voltage. Only six LEDs on each LED assembly board were wired in series so as to ensure that the constant current drivers were operated within specification. The 15 VDC to 28.5 VDC limits on the supply voltage of the Flex Imager was defined by the described LED architecture and FlexBlock drivers. Pulse width modulation was also considered for Flex Imager LED wiring but was not implemented as the LEDs were only activated for the short period around imaging operations and thus the associated power savings did not outweigh the added mass and complexity of additional hardware.

7.1. Autonomous and real-time user control

The Flex Imager was developed to operate as a fully autonomous payload or under crew-assisted control. In autonomous mode, the imager was configured to collect its nominal fluorescent and thermal images on a sequence set pre-flight. This was nominally conducted through the integration of a tablet computer connected to the various system components (cameras, relays, LEDs) through the use of a USB hub (Belkin (PSa525) 4-Port Ultra-Slim Desktop Hub). To permit operator access, the tablet was affixed to the exterior of the MDL as shown in Fig. 5.

In this configuration, the operator was able to configure and then launch the payload in autonomous mode for the research flight in question. Alternatively, should crew tending be desired (and possible) in flight, this tablet could instead serve as the operator to payload interface, allowing the operator full control over imager configuration or operation. In both cases, all collected images were saved locally to this tablet. To facilitate control further,

a second tablet was setup and appropriate communications protocols configured to permit wireless control of the payload. Both tablets were Microsoft Surface Pro tablets running Windows 8 with 4 GB RAM and 128 GB ROM. The described tablet to tablet wireless connection allowed the operator to control the payload even when it was not physically possible to be co-located with the hardware, such as that illustrated in Fig. 5 where operator control was demonstrated from the cockpit of the T-6. The wireless link established between the two tablets for real-time remote tending was a password protected ad hoc network configured on the interface tablet affixed to the MDL. The operator connected to this network using the operator controlled tablet. Once a connection was established, a remote desktop connection was launched between the two machines. Although further modifications could be incorporated into the Flex Imager for future application on-orbit, as the described design focused on operation in only parabolic, suborbital and space analog environments, no radiation protection was built into the system nor was its effect assessed.

8. Software

With the intent to minimize the operator learning curve and difficulty in further enhancing the Flex Imager, COTS software packages were chosen for both imager operations and post processing of the collected images/data. MaxIm DL version 5.23 from Diffraction Limited (Ottawa, Ontario) was utilized to control the Ascent camera and filter wheel and to process the collected images. MaxIm DL permitted both manual control of the Flex Imager as well as automated control through the scheduling of specific



Fig. 5. Wireless tablet control of the Flex Imager. The MDL mounted tablet was hardwired, to the internal USB hub and configured to distribute a wireless network (right). The tablet remained affixed to the MDL during flight, such as when the MDL was installed in the T-6 rear baggage compartment. The operator controlled tablet is connected to this configured wireless network and utilized to actively control the hardwired tablet and payload (left).

image sequences, with their respective integration times, filters, etc. Lighting control was provided through the RelayTimer R2X software package version 2.40.0.1086 from Serial Port Tool/National Control Devices. This program permitted direct interfacing with the two USB controlled relays on the relay controller boards in a manual or automatic scheduling fashion. All operational deployments of the Flex Imager also included a MSR 145 environmental datalogger from MSR Electronics (Seuzach, Switzerland) capable of collecting temperature, humidity, pressure and three-axis acceleration data at high frequency. The MSR 145 was operated using MSR software (version 5.20.03) also from MSR Electronics.

9. Thermal imaging system

So as to maximize scientific return, an A325sc thermal camera from FLIR Systems (Wilsonville, Oregon) was incorporated into the same MDL. This camera was oriented to view the same biological sample as the fluorescent imager. It is known that restricted air movement around plant leaves can result in decreased transport of heat and gases and thus influences plant photosynthesis and transpiration rates. In the spaceflight environment where only limited free convection occurs, the reduced levels of photosynthesis and transpiration may hinder plant growth (Kitaya et al., 2001, 2003). Thermal imagery of leaves undergoing parabolic flight provide a tool to better assess the influence of the microgravity environment on heat and gas exchange between the plant and the ambient environment and provide justification for the deployment of such a thermal camera within this biological imaging payload. The thermal camera utilized a 320×240 pixel uncooled microbolometer and could collect at frame rates up to 60 Hz in the $7.5 \mu\text{m}$ to $13.0 \mu\text{m}$ range. It incorporated an 18 mm focal length lens providing a 25° by 18.8° field of view, while permitting the relatively close minimum focus distance required in the tight environment of the MDL.

The thermal camera included an Ethernet port for control and data acquisition. As the Flex Imager does not utilize any Ethernet connections for any other hardware and the bulk of the available tablets do not come standard with an Ethernet port, an Ethernet to USB adapter was acquired. The StarTech.com USB 3.0 to Gigabit Ethernet adapter (Part number: USB31000S) was obtained and installed in-line with the thermal camera as indicated by Fig. 4. The A325sc thermal camera was operated using ExaminIR version 1.40.17 software from FLIR Systems.

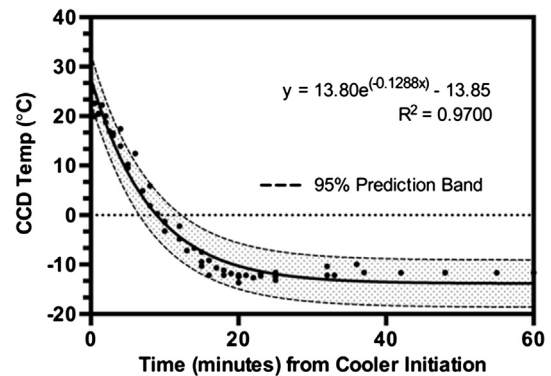


Fig. 6. Ascent CCD cooling times for five conducted tests.

10. Results and discussion

The Flex Imager has undergone testing in both the laboratory environment and also under mission relevant deployments. The laboratory tests were conducted to assess both subsystem and overall imager performance as well as define imager calibration approaches. The deployments focused on advancing the readiness of the complete imager payload while improving the operational procedures that can be incorporated into flight campaigns in any platform where the MDL form factor is accommodated. Results from these tests are discussed relative to operational deployment for actual space-related science studies.

10.1. Ascent CCD cooling time

Several tests were conducted to obtain the approximate time required for the Ascent CCD to cool to its minimum temperature set point ($\sim -12^\circ\text{C}$). These were conducted at room temperature with the initial camera/CCD temperature between 20°C and 25°C . Time zero was considered to be when the image sensor cooler was activated and the CCD temperature was monitored through MaxIm DL during the experiment. CCD temperature over time for the five conducted tests is presented in Fig. 6.

As is apparent when operating at room temperature, it took approximately 20 min for the camera to reach its minimum temperature set point. As the CCD cooler marginally overshoot the set point, a more prudent estimate of CCD temperature stabilization is 25 min. It should be noted that the relatively long period required for the CCD to drop its temperature is primarily driven by the fact that the cooler power level is increased in a stepwise fashion

(within its operations software) and thus does not immediately activate at full 100% power (this parameter is not modifiable). Fig. 6 data can also be utilized to estimate the required time to cool the CCD to other temperature set points. A test was also conducted to assess the time required for the Ascent CCD to warm from its lowest set point of approximately -12°C to a new set point of -5.0°C . The CCD reached -50°C in approximately 15 min but required a few additional minutes to stabilize ($< 0.1^{\circ}\text{C}$ changes). This data demonstrates that adjustments to CCD temperature set points, even increases, can take a moderate amount of time and must be factored in when using such imaging systems in operationally relevant environments such as proposed with the Flex Imager.

10.2. LED stabilization time and output stability

LED output decreases as LED junction temperature rises. Scientifically speaking as the goal of the Flex Imager is to assess changes in the fluorescence of reporter lines, if the excitation LED intensity changes between image sets, then comparison amongst images becomes more challenging. Although the implemented fluorescent calibration targets help alleviate some of this difficulty, ensuring LED stability between images helps simplify image processing and improves confidence in collected data sets.

An initial assessment of LED stabilization time was conducted by using the thermistor incorporated into the 40 mm LED boards. Applying manufacturer documented conversion information, the thermistor temperature measurements provided an estimate of the actual LED junction temperature. Resistance was measured across the dedicated thermistor pads during LED activation and over the first few minutes of operation and repeated several times. These basic tests demonstrated a very rapid change in LED junction temperature (from room temperature up to 55°C to 65°C in less than 1 min). Following this initial rapid increase, the temperature then slowly increased with time. In addition to indicating that the LEDs achieved approximate stabilization in a short period, these tests demonstrated that the LEDs were operating in a temperature range much below their absolute max junction temperature rating of $+150^{\circ}\text{C}$ and that the solid aluminum enclosure box was proving sufficient from a thermal mass perspective. LED temperature results were subsequently utilized with manufacturer provided data to estimate light intensity output changes. The observed temperature change from 25°C to 70°C (worst case) implies a light output change of approximately 4%.

In addition to estimating light output through the indirect measurement of LED temperature, a light meter was used to directly measure the change in LED output over time. The light sensor was co-located with the sample holder and oriented towards the excitation LED enclosure box. The nominal imager excitation LEDs were powered and left on as the light level was monitored. The light sensor was a photosynthetically active radiation (PAR) sensor (LI-COR LI-190SA) connected to a LI-COR LI-250 light meter both from LI-COR (Lincoln, Nebraska). Fig. 7 illustrates the change in light level over time. Although the light sensor was fixed in a stable position during measurement, it was not perfectly aligned with the LEDs and thus the plotted light levels should not be taken as absolute intensities and only employed as relative measures for how the LED intensity changed with time.

Similar to what was demonstrated with the LED temperature measurements, it is evident that the light levels undergo a relatively rapid initial decrease and then only slowly decrease with time. In particular, although the slope of the line in Fig. 7 is slowly decreasing over time, the LED light output is only changing by 0.5 to 0.8% per minute. This amount of change is relatively minor and still permits the extraction of useful fluorescent intensity changes from collected images. Further, as the bulk of Flex Imager imaging

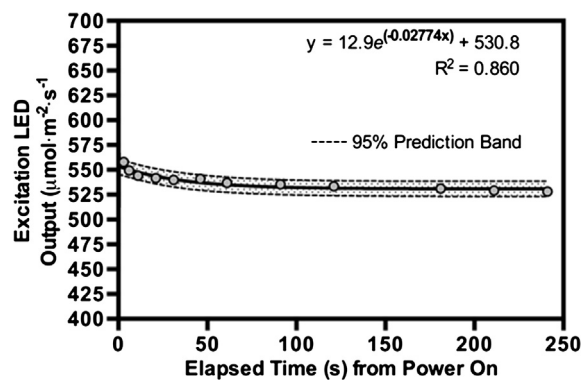


Fig. 7. Measured light level output from Flex excitation LEDs following power up. Note that the light levels only reflect relative intensities and should be used only to as a reference of change over time.

collection is done in an automated manner, each of the six nominal images is collected at a specified time following LED power up. Thus when comparing different image sets, each image with a respective filter will have been collected after the same period following LED power up. In cases where LED light output is desired to be maximally consistent, incorporation of a 30 s LED warm up period would ensure that the LED light output passed the initial period of relatively rapid decrease so that LED consistency between all collected images can be considered to be essentially the same, while balancing overall power use and added thermal load.

10.3. Image quality

Fig. 8 provides a basic representation of the image quality obtained with the Flex Imager when imaging Arabidopsis. The imager is capable of capturing details as small as trichomes (Fig. 8A) and has the versatility to capture full sized seedlings on a 10 cm Petri plate (Fig. 8B). The Flex Imager is considered a macro imaging system, similar in image size and target magnification to a typical single lens reflex camera with a macro lens for close-up imaging. The current lens system of the Flex Imager is set up to gather images of a 10 cm \times 10 cm Petri plate as per the top level requirements of Table 2. However, as seen in 8A, the level of resolution demonstrated by the Flex Imager allows for the capture of fine features that approaches a standard laboratory dissecting microscope. Also in Fig. 8, a Flex fluorescent image of a plate of seedlings expressing CaMV35s::GFP (8B) is shown in comparison to white light (8C) and fluorescent (8D) images captured with an Olympus S2X12 stereo microscope (0.5 \times lens, lowest [7 \times] zoom setting).

With the use of the six position filter wheel this high resolution imaging capability is extended to several wavelength bands of interest. Sample images from each of the respective Table 3 filters (including empty filter wheel position) are presented in Fig. 9. Although the experimental results are not elaborated here, these images were collected during a hypoxic stress experiment in a low pressure plant growth chamber.

The affixed fluorescence calibration targets (described in detail in a latter section) along with response from the planting arrangement of the experimental sample demonstrate the multispectral capabilities of the Flex Imager. In particular, image 1 passes both green and red fluorescence. Images 2 and 3 pass only GFP fluorescence, with only the top green fluorescence calibration target visible. Image 3 demonstrates segregation of red fluorescence, with only the bottom calibration target visible. A near IR fluorescence sample image is presented in image 5. In conjunction with the morphological data of image 6, detailed study of GFP and chlorophyll fluorescence can be conducted.

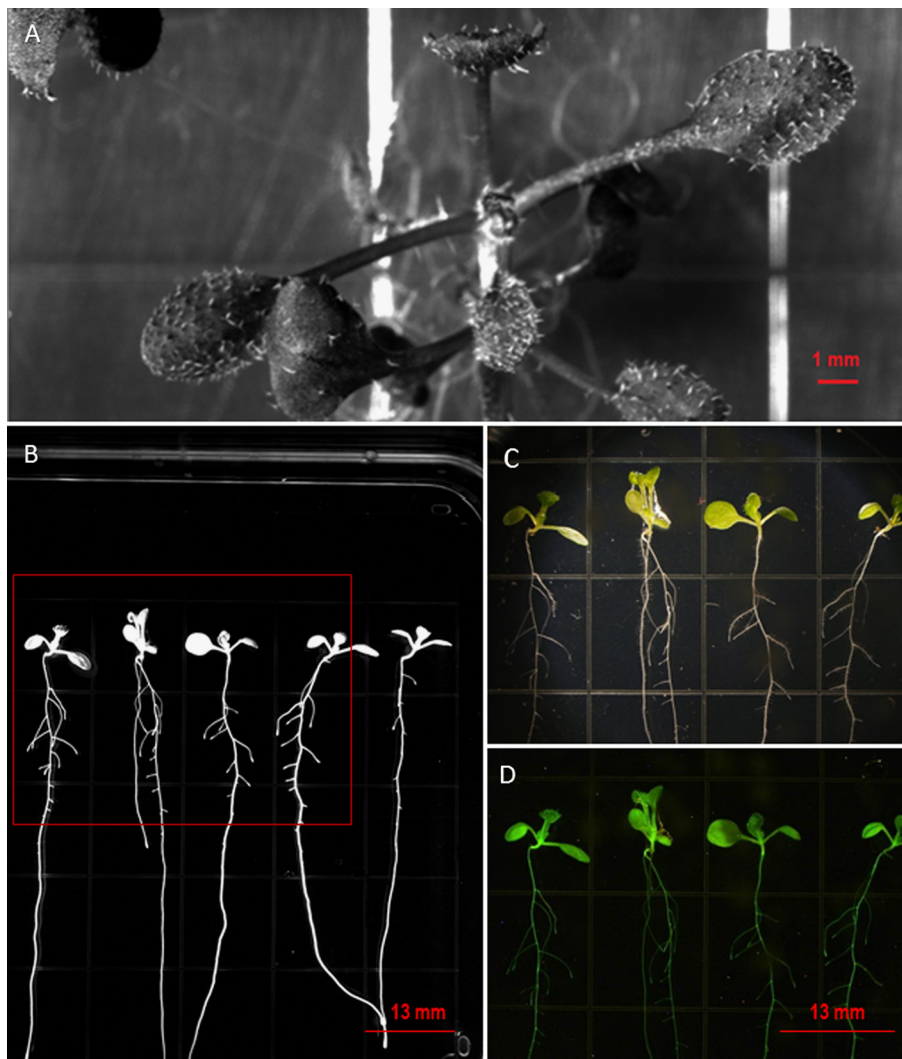


Fig. 8. Comparing Flex Imager capture to typical dissecting stereo microscope and digital camera. A) Cropped image showing achievable white light image quality of the Flex Imager; the apical meristem and leaf trichome hairs are clearly visible. B) Flex Imager full frame fluorescent capture of *Arabidopsis* plants expressing CaMV35s::GFP. C) White light image of the region of the red rectangle overlaid on the Flex image in B, captured with an Olympus S2X12 stereo microscope. The image shows the maximum frame width available for the S2X12 using the 0.5 \times lens and minimum zoom (7 \times). The resolution of the image is 2040 \times 1536. D) Fluorescent image of C captured by the S2X12. Scale bars are provided for each image. (For interpretation of the references to color in this figure legend, the reader is referred to the web version of this article.)

10.3.1. Hypoxic stress experiment description

A laboratory-based test was setup to assess several imager parameters in conjunction with the conduct of a relevant biological investigation. Controlled hypoxic stress was applied to several *Arabidopsis* reporter lines and changes to fluorescence intensity assessed over time. The induction of hypoxic stress was achieved by laying a phytigel ‘blanket’ (layer) onto the roots of several test plants. The phytigel blanket was taken from a poured phytigel plate containing no biology. The top row of the Petri plate grid was cut to ensure that when laid upon the plate of interest, that the aerial portion of the plants would remain uncovered. The phytigel plate was positioned directly over the biological test plate and a spatula used to remove the remainder of the phytigel and the blanket slowly laid onto the test plate. Both the phytigel blankets and the planted test plate incorporated 40 mL of phytigel in nominal 10 cm \times 10 cm square Petri plates. Each step was conducted in a sterilized hood and following the addition of the blanket, the biological test plate was taped closed with micropore tape. Fig. 10 displays the layout of the biological test plate including two different GFP reporters responsive to hypoxic stress in positions 1 and 3 (Adh::GFP lines “Adh196” and “AdhHx”), and a constitutively

expressing GFP reporter in position 2 (CaMV35s::GFP line “Ultra-bright”).

On June 27, 2013 at 13 : 40 a blanket was laid upon the biological test plate. The first images of this plate were taken exactly one hour later 14 : 40 with a stabilized CCD set point of +10 $^{\circ}$ C. Automated imaging was continued for approximately 4 days (until July 1 at 12 : 45) with each of the six images taken on frequency of 1 hour (initially more frequently).

10.3.2. Calibration targets

Two types of calibration targets were installed on the front of the biological test plate. The first target was employed a black gradient grid printed with a laser printer on both green and pink fluorescent Avery (Pasadena, California) High Visibility 2'' \times 4'' labels cut to size before being taped onto the front of the Petri plate. The other targets were fabricated as fluorescent bead suspensions from Duke/Thermo Fisher Scientific (Waltham, Massachusetts) green (G700) and red (R700) fluorescent bead suspensions in 1 : 25 (w/v) from which serial dilutions were made resulting in concentration sets of 1 : 25, 1 : 50, 1 : 100, 1 : 200, 1 : 400 and 1 : 800. These were then filtered and a drop of each homogenized suspension placed on nitrocellulose. The nitrocellu-

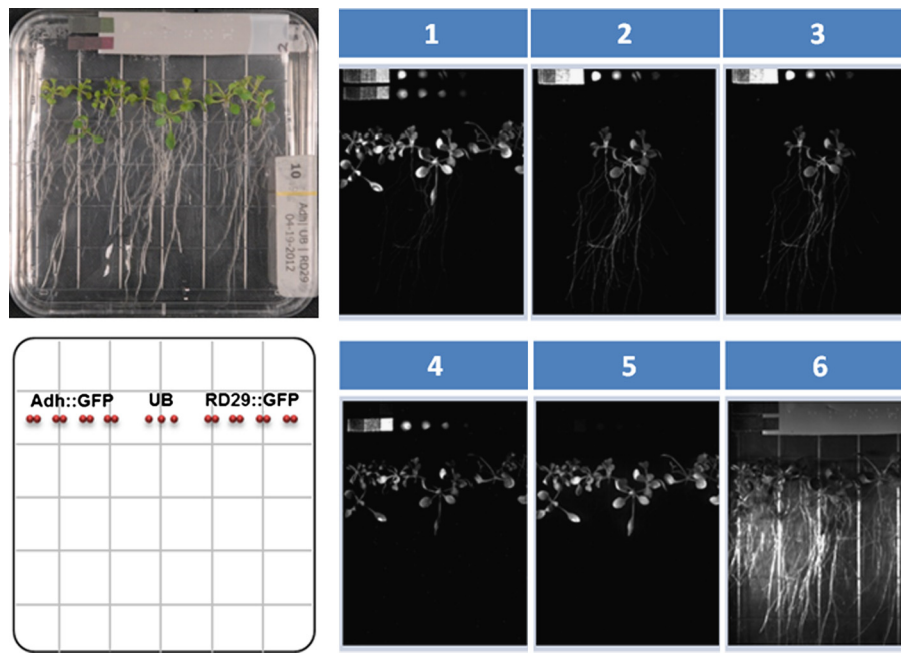


Fig. 9. Sample Flex Imager images collected for each of the respective Table 3 filters (with filter wheel position indicated). Imager calibration targets appear at the top of each image. The top and bottom calibration targets for green and red fluorescence respectively. For additional information see text. (For interpretation of the references to color in this figure legend, the reader is referred to the web version of this article.)

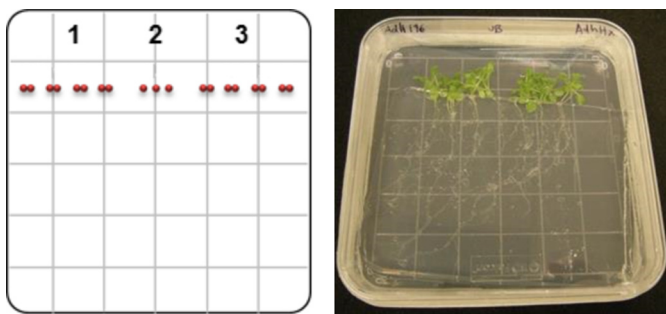


Fig. 10. Approximate layout of biological test plate (left). Positions 1, 2, 3 correspond to the Adh196, Ultrabright and AdhHx reporters respectively. Pre-experiment photograph of the test plate (right).

lose was then trimmed to size and taped to the front of the Petri plate.

10.3.3. Image stability

Calibration targets should maintain constant fluorescence when instrument parameters (in particular the LED output) remain stable. Thus fluorescence from the employed calibration targets was utilized to assess image stability by defining regions of interest (a rectangular image area x by y pixels in size) covering the geometrical location of the calibration target and assessing pixel intensity changes over time. LEDs were powered on for 30 s prior to each automated hourly image collection sequence. The average pixel intensity over the entire region of interest (single image) was output for each hourly time point. As evident from Fig. 11, the fluorescence intensity measured from both types of calibration targets was quite stable over the duration of the experiment.

As an added verification of camera stability, initial and post-experiment 10 s exposure dark images (no filter) were compared and shown to be essentially the same. The average pixel count over the entire image of the initial dark image was 1005.09 with a standard deviation of 130.35 and for the post-experiment image 1010.15 with standard deviation of 131.54.

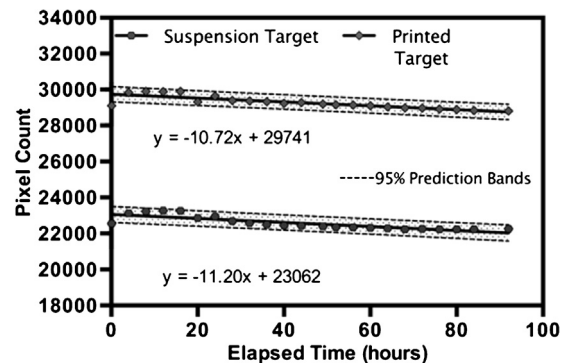


Fig. 11. Plot of average pixel intensities (raw counts) of the printed label and bead suspension fluorescent calibration targets over time.

10.3.4. Hypoxic stress imaging results

The capacity of the Flex Imager to measure changes to the fluorescence of the biological samples was also conducted. Regions of interest from each image were defined on key structures of the Ultrabright and Adh reporter lines. The selected regions of interest were boxes of X by Y pixels drawn around e.g. roots, root-tips, stems and other areas of interest. Fig. 12 displays the initial and final fluorescent images (filter 2, same screen stretch) of the biological test plate. It is visually evident that both the left Adh196 and AdhHx show an increase in fluorescence over time.

A comparison of the fluorescence intensities displayed in percent change over time, of the specific regions of interest defined on the roots of each respective reporter, are displayed in Fig. 13. In comparison to the Ultrabrights, both versions of the Adh reporters showed an increase in their fluorescence over time in the presence of hypoxic stress. Localized hypoxia was created by covering a section of the roots growing along the surface of the base layer of phytigel with an additional layer of solidified gel. This blanket over the roots slowly reduces the amount of available oxygen in the region, which induces the transcription of the Adh gene and any reporter gene constructed with the Adh promoter region (Paul et al., 2001).

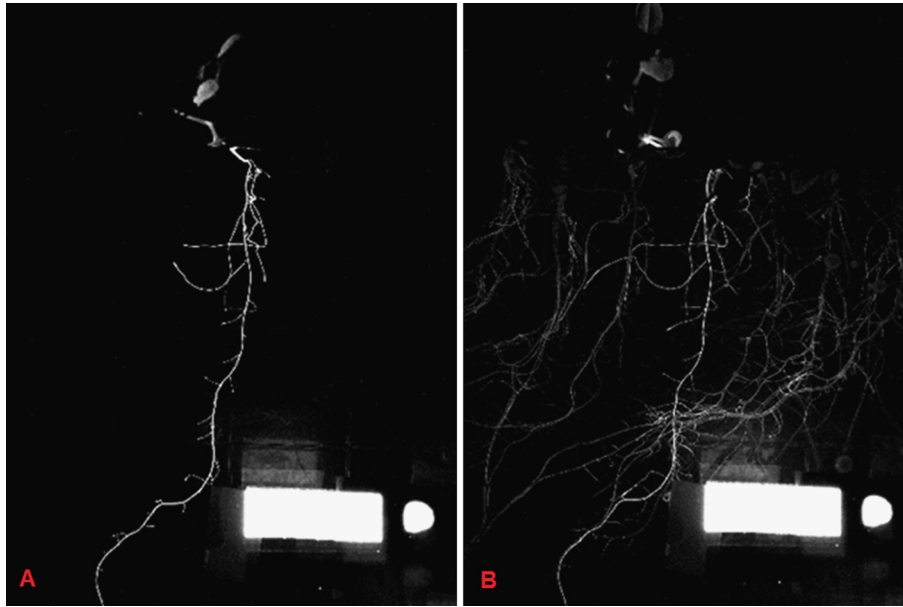


Fig. 12. Initial $T = 0$ hour (A) and final $T = 92$ hours (B) test plate fluorescent images (pixel intensity screen stretch 500–4000). Note that the calibration target is saturated in these images to better display change in fluorescence of test plants. As evident, Adh196 and AdhHx samples show increased fluorescence in the later $T = 92$ hours image.

10.4. Deployments

The Flex Imager, or in some cases earlier iterations of its design have been deployed in a number of relevant scientific or mission relevant operational environments. Basic descriptions of these deployments including any imager configuration differences are described.

10.4.1. Parabolic flight campaign

The initial parabolic Flex Imager employed a color Ascent A8050 camera. This camera was utilized in conjunction with a C-mount lens, lens mount and imaging filter. The single imaging filter (515 nm) was installed in a machine shop modified Ascent camera to C-mount lens adapter (modified specifically to hold 25 mm diameter, 5 mm thick optical filters). A Kowa LM16XC (Tokyo, Japan) C-mount lens was utilized and installed on an Ascent to C-mount lens adapter (Part number: 100163) from Apogee Imaging Systems. Although the image projection from C-mount lenses do not normally cover the entire CCD area of large area CCDs, the LM16XC is in the family of C-mounted lenses with large image circles. The lens included a 16 mm focal length and with a minimum focusing distance of 0.1 m, permitted focusing at the short path lengths within a MDL. Two 1 mm C-mount lens spacer rings from 1stVision (Andover, Massachusetts) were employed to ensure optimal image focus for this fixed configuration.

This initial Flex Imager configuration flew on four parabolic flights as part of NASA's February to March 2013 flight campaign. The Flex Imager was integrated into NASA Kennedy Space Center's FASTRACK platform as shown in Fig. 14. The MDL tray was installed in the bottom MDL of FASTRACK and connected to the experimental platform's 28 VDC source power. A laptop was installed on the top of the FASTRACK platform and allowed researcher control of the Flex Imager and data collection throughout the flight.

Each of the four flights on the ZeroG Corporation (Arlington, Virginia) Boeing 727-200 targeted 40 parabolas and was of an approximate duration of two hours. The Flex Imager hardware had a mass of 15.1 lb and when integrated into the full MDL the total payload mass (i.e. including the MDL tray) was 18.8 lb.

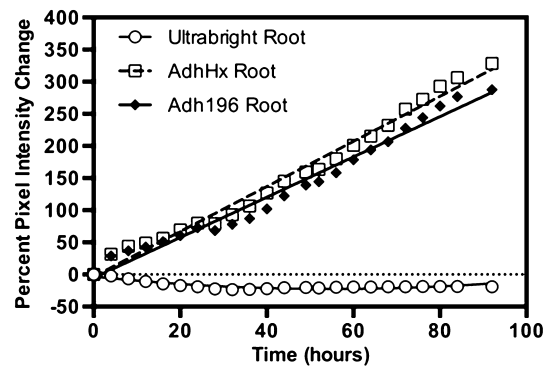


Fig. 13. Percent change in pixel intensities over time of the various reporters.

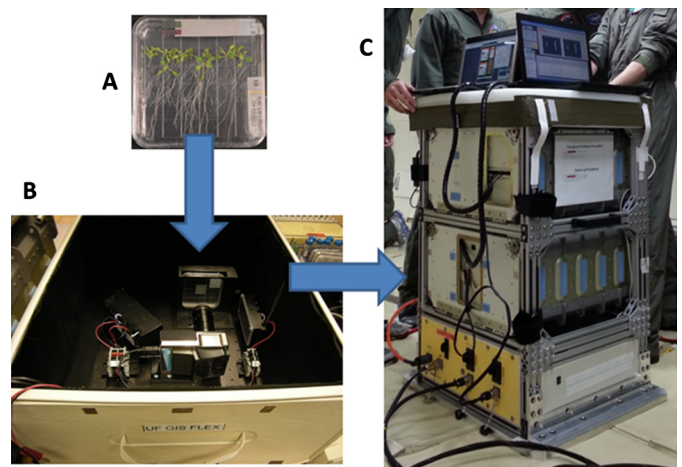


Fig. 14. Arabidopsis on Petri plate (A) installed in the Flex Imager within MDL tray (B) installed in the lower MDL drawer within FASTRACK (C) for parabolic flights.

10.4.2. Hypobaric chamber experiments

Prior to this deployment there was some uncertainty whether the fluorescent camera could operate at low pressure as no manufacturer information was available from this regard. The low

Table 4

Measured Flex thermoelectric cooler usage during low pressure experiments. These tests were conducted within a MDL tray, but not installed within a MDL.

Pressure (kPa)	Chamber temp. (°C)	CCD set temp. (°C)	Stabilized TEC power (%)	Cover on imager (Y/N)
25	25	5	Not possible to maintain	Y ^a
25	25	10	71%	Y ^a
10	25	10	Not possible to maintain	Y ^a
10	25	15	68%	Y ^a
10	22	15	26–27%	N
5	22	15	30%	N
98	22	15	14%	N

^a Due to the black cloth placed over the top of the MDL tray (attached with Velcro as it was during the parabolic flights) the imager reached a very high temperature. In particular, measured temperature on the back of the biological sample holder was 32 °C. Thus in the subsequent experiments the black cloth cover was removed.

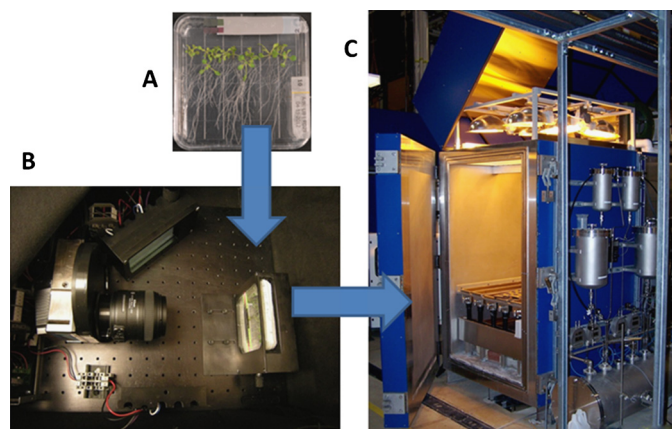


Fig. 15. Biological sample (A) installed in the Flex Imager within a MDL tray (B) and then installed in a large low pressure chamber (C) for hypobaric experiments.

pressure imaging experiments were conducted at the Controlled Environment Systems Research Facility at the University of Guelph at the end of April, 2013. They involved the deployment of the Flex Imager with the monochrome camera with the filter wheel and F-mount lens as displayed in Fig. 15 (no tablet control or thermal camera).

From a hardware perspective the tests confirmed that the Flex Imager could function nominally at low pressure. In particular, the imager operated at 5 kPa and for approximately 24 hours without issue. Further, several long duration (48 hours or more) tests at 10 kPa were conducted and as at 5 kPa, the imager functioned nominally. The low pressures drove higher thermoelectric cooler cooling loads. At normal (1 atm) atmospheric pressure, the Ascent cooler can bring the CCD down to -10°C to -12°C . As seen in Table 4, at reduced pressures, the cooler could not achieve the same low CCD temperatures. For example, even at 25 kPa, the cooler could not maintain a CCD temperature as low as $+5^{\circ}\text{C}$.

10.4.3. T-6 flight campaign

The full-up Flex Imager configuration including monochrome camera, filter wheel, F-mount lens as well as tablet to tablet wireless control (and thermal camera) was flown during a June, 2013 T-6 flight campaign. Two flights were flown with the imager installed within the T-6 baggage compartment as shown in Fig. 16.

Flights were conducted primarily to test the imager under flight conditions and to draw on the operational lessons learned to benefit the continued development of the imager for suborbital flight. The flights demonstrated that tablet to tablet wireless connectivity proved to be a valid solution even with the Flex Imager installed in the fully closed baggage compartment. If an operator is to provide real-time control of the imager using the tablet and stylus during flight, as conducted during the T-6 campaign, a top-layer graphical user interface with larger push buttons should be developed as in

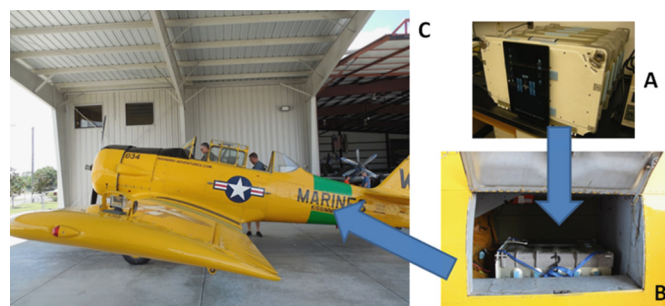


Fig. 16. T-6 flight campaign. Integrated Flex and thermal imagers contained within a MDL (A) mounted into the T-6 baggage compartment (B) and controlled through a wireless tablet from the front seat (C).

flight vibration and maneuvers makes accessing the nominal software package menu bars somewhat difficult. The flown payload (integrated fluorescent and thermal imaging) including the front mounted tablet and including the MDL tray had a total mass of 23.6 lb. When installed in the actual MDL for installation into the T-6 baggage compartment the full payload mass was 38.0 lb.

11. Conclusions and future

The Flex Imager is a flexible imaging payload for use in the assessment of plant responses to novel environments, with particular emphasis on upcoming suborbital flight opportunities. The flexibility of the imager stems from its standard MDL sizing, multi-hole baseplate permitting adaptable component positioning, its use of COTS hardware and software and standard imaging data output format. This flexibility facilitates the field change-out or upgrade of specific components, an important consideration for the greater flight rates expected by the forthcoming suborbital launch industry. Indeed, with short turnarounds between flights possible, flexible payloads like the Flex Imager will permit researchers to make rapid modifications to their payloads based upon lessons learned in earlier flights. In addition to the collection of relevant scientific data in the assessment of plant responses to novel environments, the Flex Imager has been tested in several relevant operational environments that aid in its readiness for suborbital flight. Iterations of the Flex Imager payload have flown in parabolic flight campaigns (727–200), on T-6 tests flights as well as been used in low-pressure research chambers. The current payload remains focused on fluorescence imaging but also incorporates a thermal camera that collects real-time information on the same biological sample. Based upon past imager developments the Flex Imager also incorporates a cooled CCD camera, filter wheel and suite of five imaging filters, permitting consistent collection of fluorescent images at various wavelengths of interest. Characterization of the imager has included assessment of excitation LED stability, imaging stability as well as laboratory-based hypoxic stress induced studies of relevant biological samples. The Flex Imager has been demonstrated to capture appropriate biological signals over timeframes

and operational deployments suitable for science experiments in spaceflight and spaceflight related venues.

Based upon the described lab testing and operational experience, a number of design improvements are likely to be incorporated into the Flex Imager to further its readiness for multiple deployment opportunities, including suborbital flights and space analogs/flight-related platforms. In particular, an improved software interface is being developed. This improved graphical user interface will simplify the operator control of the imager and better permit flight test engineers to more easily operate the payload, in particular if hardware anomalies should occur. Software alarms and simplified reset functionality will also be included. Custom MDL front panels will be fabricated that will better permit heat exchange out of the MDL drawer. These front panels will also incorporate cable passes and flexible power connectors. From the perspective of improving fluorescent image quality, improved calibration targets will be investigated so as to reduce the fluorescent light from the targets straying onto the biological sample and subsequently influencing the perceived fluorescence of the regions of interest. A redundant imager is also being manufactured so as to provide a flight ready backup should issues arise during any upcoming flight campaign. The second imager will also be utilized for ground control imaging and permit real-time on-ground troubleshooting during longer duration flight campaigns.

Acknowledgements

This work was partly supported by a UCF-UF Space Research Initiative Award (66014402), the NASA Flight Opportunities Office, NASA grants NNX13AM46G and NNX12AN69G, as well as the NASA Postdoctoral Program (NPP) (NNH06CC03B) for partial support of Thomas Graham's activities. The NPP is administered by Oak Ridge Associated Universities through a contract with NASA. The authors would also like to acknowledge the assistance of representatives from Earthrise Space Inc. in the design and fabrication of several mechanical components included in the described payload. Talal Abboud is thanked for providing the samples images from the TIS-III and TIS-IV imagers in Table 1. Eric Schultz is acknowledged for fabricating the fluorescent bead suspension calibration targets. Trevor Murdoch is acknowledged for his large role in the development of the early GIS imaging systems and supplied the excitation filter used in this imager.

References

- Abboud, T., Berinstain, A., Bamsey, M., Ferl, R., Paul, A.-L., Graham, T., et al., 2013a. Multispectral plant health imaging system for space biology and hypobaric plant growth studies. *Insciences J.*
- Abboud, T., Bamsey, M., Paul, A.-L., Graham, T., Braham, S., Noumeir, R., et al., 2013b. Deployment of a fully-automated green fluorescent protein imaging system in a High Arctic autonomous greenhouse. *Sensors* 13, 3530–3548.
- Bingham, G.E., Topham, T.S., Taylor, A., Podolsky, I.G., Levinskikh, M.A., Sychev, V.N., 2003. Lada: ISS plant growth technology checkout. ICES, SAE Technical Paper, 2003-01-2613.
- Boeing, 1997. Middeck interface definition document. Rev B ed., Boeing, Downey, CA.
- Brinckmann, E., 2005. ESA hardware for plant research on the International Space Station. *Adv. Space Res.* 36, 1162–1166.
- Evans, C.A., Robinson, J.A., Tate-Brown, J., Thumm, T., Crespo-Richey, J., Baumann, D., et al., 2009. International Space Station science research accomplishments during the assembly years: an analysis of results from 2000–2008, NASA, NASA JSC.
- Hoehn, A., Chamberlain, D.J., Forsyth, S.W., Gifford, K., Hanna, D.S., Horner, M.B., et al., 1996. Plant Generic bioprocessing apparatus: a plant growth facility for space flight biotechnology research. In: Kaldeich, B. (Ed.), *Life Sciences Research in Space, Proceedings of the Sixth European Symposium*. ESA, Trondheim, Norway.
- Johnsson, A., Solheim, B.G.B., Iversen, T.-H., 2009. Gravity amplifies and microgravity decreases circumnutations in *Arabidopsis thaliana* stems: results from a space experiment. *New Phytol.* 182, 621–629.
- Kitaya, Y., Kawai, M., Tsuruyama, J., Takahashi, H., Tani, A., Goto, E., et al., 2001. The effect of gravity on surface temperature and net photosynthetic rate of plant leaves. *Adv. Space Res.* 28, 659–664.
- Kitaya, Y., Kawai, M., Tsuruyama, J., Takahashi, H., Tani, A., Goto, E., et al., 2003. The effect of gravity on surface temperatures of plant leaves. *Plant Cell Environ.* 26, 497–503.
- Knott, W.M., Sager, J.C., 1991. Monitoring and control technologies for bioregenerative life support systems/CELSS, Technology 2000, NASA-CP-3109, NASA Headquarters, pp. 161–167.
- Krause, G.H., Weis, E., 1991. Chlorophyll fluorescence and photosynthesis: the basics. *Annu. Rev. Plant Physiol. Plant Mol. Biol.* 42, 313–349.
- Levine, H.G., Cox, D.R., Reed, D.W., Mortenson, T.E., Shellack, J.L., Wells, H.W., et al., 2009. The Advanced Biological Research System (ABRS): a single middeck payload for conducting biological experimentation on the International Space Station. in: 47th AIAA Aerospace Sciences Meeting, AIAA 2009-416.
- Link, B.M., Durst, S.J., Zhou, W., Stanković, B., 2003. Seed-to-seed growth of *Arabidopsis thaliana* on the international space station. *Adv. Space Res.* 31, 2237–2243.
- Maxwell, K., Johnson, G.N., 2000. Chlorophyll fluorescence – a practical guide. *J. Exp. Bot.* 51, 659–668.
- Morrow, R.C., Crabb, T.M., 2000. Biomass Production System (BPS) plant growth unit. *Adv. Space Res.* 26, 289–298.
- NASA, 1984. Orbiter middeck/payload standard interfaces control document, NASA JSC, Houston, TX.
- Paul, A.-L., Daugherty, C.J., Bihn, E.A., Chapman, D.K., Norwood, K.L.L., Ferl, R.J., 2001. Transgene expression patterns indicate that spaceflight affects stress signal perception and transduction in *Arabidopsis*. *Plant Physiol.* 126, 613–621.
- Paul, A.-L., Murdoch, T., Ferl, E., Levine, H.G., Ferl, R., 2003. The TAGES imaging system: optimizing a green fluorescent protein imaging system for plants. SAE Technical Paper, 2003-01-2477.
- Paul, A.-L., Bamsey, M., Berinstain, A., Braham, S., Neron, P., Murdoch, T., et al., 2008. Deployment of a prototype plant GFP imager at the Arthur Clarke Mars greenhouse at the Haughton Mars Project. *Sensors* 8, 2762–2773.
- Paul, A.-L., Amalfitano, C.E., Ferl, R.J., 2012. Plant growth strategies are remodeled by spaceflight. *BMC Plant Biol.* 12, 232.
- Paul, A.-L., Zupanska, A.K., Schultz, E.R., Ferl, R.J., 2013. Organ-specific remodeling of the *Arabidopsis* transcriptome in response to spaceflight. *BMC Plant Biol.* 13, 112.
- Stewart Jr., C.N., 2001. The utility of green fluorescent protein in transgenic plants. *Plant Cell Rep.* 20, 376–382.
- Stutte, G.W., Monje, O., Goins, G.D., Tripathy, B.C., 2005. Microgravity effects on thylakoid, single leaf, and whole canopy photosynthesis of dwarf wheat. *Planta* 223, 46–56.
- Sychev, V.N., Levinskikh, M.A., Gostimsky, S.A., Bingham, G.E., Podolsky, I.G., 2007. Spaceflight effects on consecutive generations of peas grown onboard the Russian segment of the International Space Station. *Acta Astronaut.* 60, 426–432.
- Virgin-Galactic, 2011. Virgin Galactic Payload User's Guide.
- XCOR-Aerospace, 2012. XCOR Lynx Payload User's Guide.
- Zhang, J., Campbell, R.E., Ting, A.Y., Tsien, R.Y., 2002. Creating new fluorescent probes for cell biology. *Nat. Rev. Mol. Cell Biol.* 3, 906–918.
- Zhou, W., 2005. Advanced ASTROCULTURE plant growth unit: capabilities and performances. SAE Technical Paper, 2005-01-2840. ICES.